Tellus SERIES B CHEMICAL AND PHYSICAL METEOROLOGY
PUBLISHED BY THE INTERNATIONAL METEOROLOGICAL INSTITUTE IN STOCKHOLM

Tellus (2008), 60B, 674–684
Printed in Singapore. All rights reserved

TELLUS

Seasonal variations in the isotopic composition of near-surface water vapour in the eastern Mediterranean

By ALON ANGERT[1], JUNG-EUN LEE[2] and DAN YAKIR[1]*, [1]*Department of Environmental Sciences and Energy Research, The Weizmann Institute of Science, Rehovot 76100, Israel;* [2]*Berkeley Atmospheric Sciences Center, University of California, Berkeley, CA 94720-4767, USA*

(Manuscript 28 November 2006; in final form 18 March 2008)

ABSTRACT

Although the isotopic composition of precipitation is widely used in global climate change studies, use of water vapour isotopes is considerably more limited. Here we present the results from 9 yr of atmospheric vapour measurements in the Eastern Mediterranean, at a site in Israel. The measurements show a strong mean seasonal cycle of about 4‰ in ^{18}O (peaking around July). This seasonality could not be adequately explained by changes in surface interactions or in air mass trajectories, as usually invoked for variations in local precipitation. We could explain this cycle only as a combination of three components: (1) rainout effects; (2) temperature and relative humidity control of the initial vapour and (3) seasonal variations in the vertical mixing across the top of the planetary boundary layer. This last component is emphasized in the current study, and it was shown to be a significant factor in the seasonal cycle features. The measurements were also compared with an isotope-enabled GCM (CAM2) run, which exhibited a markedly different seasonal cycle. Such comparisons with vapour isotopes data could help in constraining models better.

1. Introduction

The abundance of ^{18}O and deuterium in the present and past precipitation has proven to be an important tool in Earth systems science. The stable isotopologues (chemical species that differ only in the isotopic composition of their molecules) of water ($H_2{}^{16}O$, $HD^{16}O$, $H_2{}^{18}O$, $H_2{}^{17}O$) have different saturation vapour pressures and different diffusion rates; therefore, the isotopic composition of precipitation integrates the effects of these processes over the life cycle of water in the atmosphere. The processes governing this life cycle include evaporation at the surface, vertical and lateral transport and mixing in the atmosphere, recycling by ecosystems, in situ condensation and evaporation during cloud formation and removal as rain or snow (Dansgaard, 1964; Craig and Gordon, 1965; Jouzel and Merlivat, 1984; Gat et al., 1996).Insights into these processes can be gained by studying the isotopic composition of atmospheric water.

The ratios of stable isotopes are usually presented in the normalized 'delta notation' ($\delta^{18}O$, δD, where $\delta = R_{samle}/R_{standard} - 1$ in ‰, R is $^{18}O/^{16}O$ for $\delta^{18}O$ or $^{2}H/^{1}H$ for δD, and the standard is V-SMOW), and an additional important variable, termed deuterium excess (d), is calculated from the relationships between $\delta^{18}O$ and δD, and is defined as $d = \delta D - 8\delta^{18}O$ (Dansgaard, 1964). The deuterium excess is mainly determined by the relative contributions of kinetic versus equilibrium isotopic exchanges, which in turn, depend on the evaporation rates and at low temperatures on the super saturation in ice formation (Merlivat and Jouzel, 1979). Whereas interannual variations in climate and precipitation have been compiled and are well documented (for the time period 1870–present e.g. Kalnay et al., 1996; Dai et al., 1997; Chen et al., 2002), there is a shorter (1961–present) and much sparser record of precipitation isotopes, and almost no record of the isotopic composition in atmospheric water vapour. The principal and comprehensive source of contemporary water isotope observations is the IAEA/WMO global network of isotope in precipitation (GNIP; IAEA 2001; http://isohis.iaea.org/GNIP.asp). These observations are summarized by Rozanski and Sonntag (1982).

In Israel, studies of isotopes in precipitation began in 1960 (Gat and Dansgaard, 1972; Gat et al., 1994) and have continued, with varying temporal and spatial resolutions, to date (Levin et al., 1980; Leguy et al., 1983; Gat, 1987; Goodfriend et al., 1989; Ayalon et al., 1998; Gat et al., 2001). Vapour sampling at a single site was performed systematically from January 1969 to

*Corresponding author.
e-mail: dan.yakir@weizmann.ac.il
DOI: 10.1111/j.1600-0889.2008.00357.x

the end of October 1970 (Tzur, 1971), and from December 1997 until present (Gat, Yam and Yakir, unpublished results).

Precipitation in Israel occurs primarily during the winter months and is characterized by a d value larger than that associated with the global meteoric water line (GMWL) and close to $d = 20‰$, on average, and a slope that is very similar to that of the GMWL (Gat et al., 1994). From 1961 to 1990, at the GNIP station Bet-Dagan, which has a seasonal average precipitation of 543 ± 164 mm, the amount-weighted average of the isotopic composition of precipitation was $\delta^{18}O = -4.70 \pm 0.60‰$ ($\delta^{18}O = -5.15‰$ for the mid-winter months of December–March; Gat et al., 1994). Although there is a residual correlation of the data with the amount of precipitation, both in monthly and annual averages, it is often masked by the large scatter due to other causes. It was found, however, that an important factor governing the isotope composition of the precipitation (both the δ-values and the d) is the synoptic history of the air masses concerned (Leguy et al., 1983; Gat et al., 1994, 1996), including the rainout history along the flow path. Local rain intensity did not have a strong effect on its isotopic composition (Gat et al., 2001).

Most of the previous works discussed above, focused on isotopes in precipitation and to a much smaller extent on water vapour isotopes near the surface. Observations of the isotopic composition of tropospheric water vapour are rare (Ehhalt, 1974; Rozanski and Sonntag, 1982; Lee et al., 2005), but they are important for three main reasons:

(1) The advantage over precipitation isotopes: Measurements of water vapour isotopes, in contrast to rain water, can be done across different seasons and synoptic situations and are not limited only to rainy days. This advantage of measuring water vapour over rain is particularly important in regions such as the eastern Mediterranean (EM), where rain is absent for about half of the year.

(2) Constraining GCMs: The observed spatial and temporal variations of precipitation isotopes can be used to track the water cycle, and this, in turn, can be used to constrain global circulation models (GCMs). However, such attempts have resulted in only modest success (Hoffmann et al., 2000) because they relied on the limited available data, mostly from rain water analyses. In addition to the temporal limitation mentioned above, this is also problematic since a large part of the isotopic information contained in a newly formed rain-drop is lost as the rain-drop falls and exchanges isotopes with the vapour at different levels (Bolin, 1958). These isotopic exchanges will also have an effect on the vapour with which the rain-drop equilibrates.

(3) Constraining estimates of water and carbon fluxes from plants: The isotopic composition of oxygen in atmospheric O_2 and CO_2 has been proposed as a tracer of land vegetation activity and is expected to serve as a powerful tool for tracing the feedback from vegetation activity to climate through the water and carbon cycles (e.g. Farquhar et al., 1993; Bender et al., 1994). A key parameter in these applications is the isotopic composition of leaf water (as a result of the massive CO_2/H_2O isotopic exchange in leaves and the production of O_2 from leaf water). Estimating the isotopic enrichment in leaf water, in turn, critically depends on knowledge of the isotopic composition of atmospheric water vapour. This parameter, however, is seldom measured and is currently one of the major uncertainties in understanding variations in leaf water oxygen content and, in turn, in using the ^{18}O content of atmospheric O_2 and CO_2 as a useful tool.

In the current study, we performed a case study by tracking the water vapour isotopic composition at a site in Israel over 9 yr (1998–2006). The results from this study were compared with model results from an isotope-enabled atmospheric GCM. An advantage of our study site is that precipitation isotopes in the eastern Mediterranean (as well as in Europe and other neighbouring areas) and some of the processes that influence them were well studied, as indicated above. Thus, this study aimed at going beyond the more studied relationships of vapour and rain-drop equilibration during rain events and the expected effect of rain-out along the trajectory on the isotopes' seasonal cycle.

2. Methods

2.1. Vapour collection and isotopic measurements

'The sampling site' was the Environmental Sciences building rooftop (76 m asl, ~6 m above ground) at the Weizmann Institute of Science in Rehovot, Israel (31°53′ N, 34°49′E, see map in Fig. 1), on the eastern Mediterranean (EM). The site's climate is a typical Mediterranean one, with mild winters and warm and dry summers (Fig. 2). Sampling took place usually twice a week

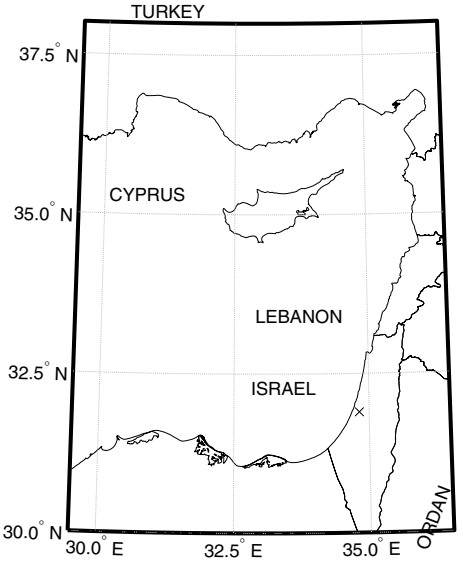

Fig. 1. Map of the study area, showing the sampling site in Rehovot, Israel.

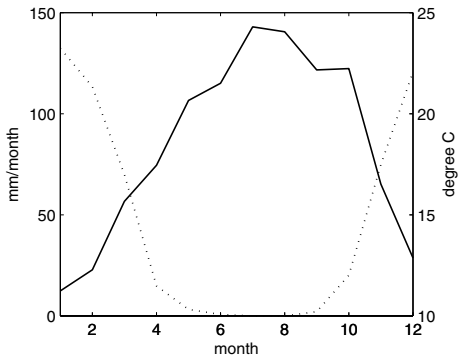

Fig. 2. Climatological monthly precipitation (dotted line, data from the Israel Meteorology Service for the nearby Hulda, 31°49′N,34°52′E, station), and air temperature (solid line, data from the Israeli Ministry for Environmental protection for the Rehovot station).

although some gaps in the data exist. Air temperature was taken from a nearby metrological station at Rehovot.

Air was pumped by a vacuum pump through an inverted funnel (i.e. facing the ground to prevent liquid moisture intake) through 6 mm OD plastic tubing (Bev-A-Line) and a 10 mm OD Pyrex spiral cold trap (70 ml volume), immersed in ethanol–dry ice slash at about –80 °C. The flow rate was 4 LPM, and moisture was collected (2–4 ml) in the trap for 5–9 h starting at 8 a.m. At the end of the sampling period, the trap was sealed at its two ends and warmed to room temperature. Water was mixed across the trap before decanting into a 5 ml vial and sealed. An aliquot of 0.5 ml each of water sample was placed in a 7 ml tube, degassed under vacuum to 10^{-5} Torr, and known CO_2 at 250 Torr was added for equilibration. Equilibration was carried out overnight at 29.5 °C on a shaker, after which CO_2 was cryogenically collected and sealed in a Pyrex tube for the isotopic analysis using an automatic manifold on a Finnigan MAT 250 mass spectrometer. Every other sample was also used for hydrogen isotopic composition. Aliquots of 2.8 μl were added with 90 mg Zn (super dried) into a dry tube connected to a vacuum line. After degassing, the tube was sealed and heated to 497 °C for 60 min and cooled to room temperature before isotopic analysis on the same mass spectrometer. The precision of the isotopic analysis was 0.1 ‰ and 1‰ for oxygen and hydrogen, respectively, and the precision of deuterium excess was 1.8‰.

The monthly mean isotopic values were calculated by a simple average and not by moisture amount weighted averaging. This was done since we are interested in directly determining the isotopic ratios and not in integrating isotopic values into flux (isoflux) or in the absolute mass balance.

2.2. Modelling—isotopic enabled GCM

The water isotope module is based on the national center for atmospheric research (NCAR), community atmospheric model, version 2 (CAM2) at T42 resolution (approximately 2.815° × 2.815°). The vertical grid has 26 levels from the surface up to 2 hPa. Details of the model are documented in Collins et al. (2002). The model is forced by the observed climatological monthly mean sea surface temperatures (from the NCEP reanalysis). Water isotopes were incorporated into CAM2, similarly to previous model studies (e.g., Jouzel, et al., 1987; Hoffmann, 1998; Mathieu et al., 2002), with fractionation associated with evaporation at the surface as well as with cloud processes. The kinetic fractionation factor and subcloud relative humidity were set to the values proposed by Mathieu et al. (2002). Details of the model are described in Lee (2005).

NCAR CAM2 uses the (Zhang and McFarlane (1995) deep convection scheme, which parameterizes the effect of the convective cloud system on large-scale (grid-scale) conditions. The vertical water vapour budget follows the entrainment, detrainment, updraft and downdraft of the air mass, as parameterized by the convective scheme, and isotopic fractionation is invoked whenever a phase transition occurs.

The isotopic composition of the atmospheric vapour is initialized with -600‰ for δD and -80‰ for δ^{18}O; soil water is initialized using the Dansgaard relationship (Dansgaard, 1964), relating surface temperature and the isotopic composition of the precipitation, which is the source for the soil water. The model was integrated for 10 yr, and the fields of the last 8 yr were used for analysis (i.e. the first 2 yr were used as spin-up, to enable the model to reach equilibrium).

3. Results and discussion

3.1. Seasonal variations in the vapour isotopic composition

The data collected over the years 1998–2006 are presented in Fig. 3. The isotopic composition of the vapour samples showed a marked seasonal cycle, consistent with previous, much shorter observation record in the mean vapour data, which did not provide an explanation for seasonal cycle (Tzur, 1971). In summer, oxygen isotopic composition varied between -13 and -9‰ with a d in the range $5‰ \leq d \leq 22‰$. Winter values were more scattered, in the range $-10‰ \leq \delta^{18}O \leq -18‰$, with d values of up to +40‰. The data from spring and autumn follow a trend line between these two seasonal values. Samples taken from rainy days often exhibited the most extreme values. The correlation coefficient between the air temperature and δ^{18}O was $R^2 = 0.38$, and the slope was 0.19 (permil/°C). The observed relationship between δD and δ^{18}O was $\delta D = 4.7\ \delta^{18}O + 0.45$ ($R^2 = 0.65$). The monthly mean (averaged over all sampling years) for δD, δ^{18}O and d values are presented in Fig. 4. In the rest of the paper, we focus on the variations in δ^{18}O in representing the seasonal patterns, and the d parameter will be used where the variations in δ^{18}O and δD are not linearly correlated.

Seasonal variability similar to that in vapour, was observed in the isotopic composition of precipitation in Israel but only

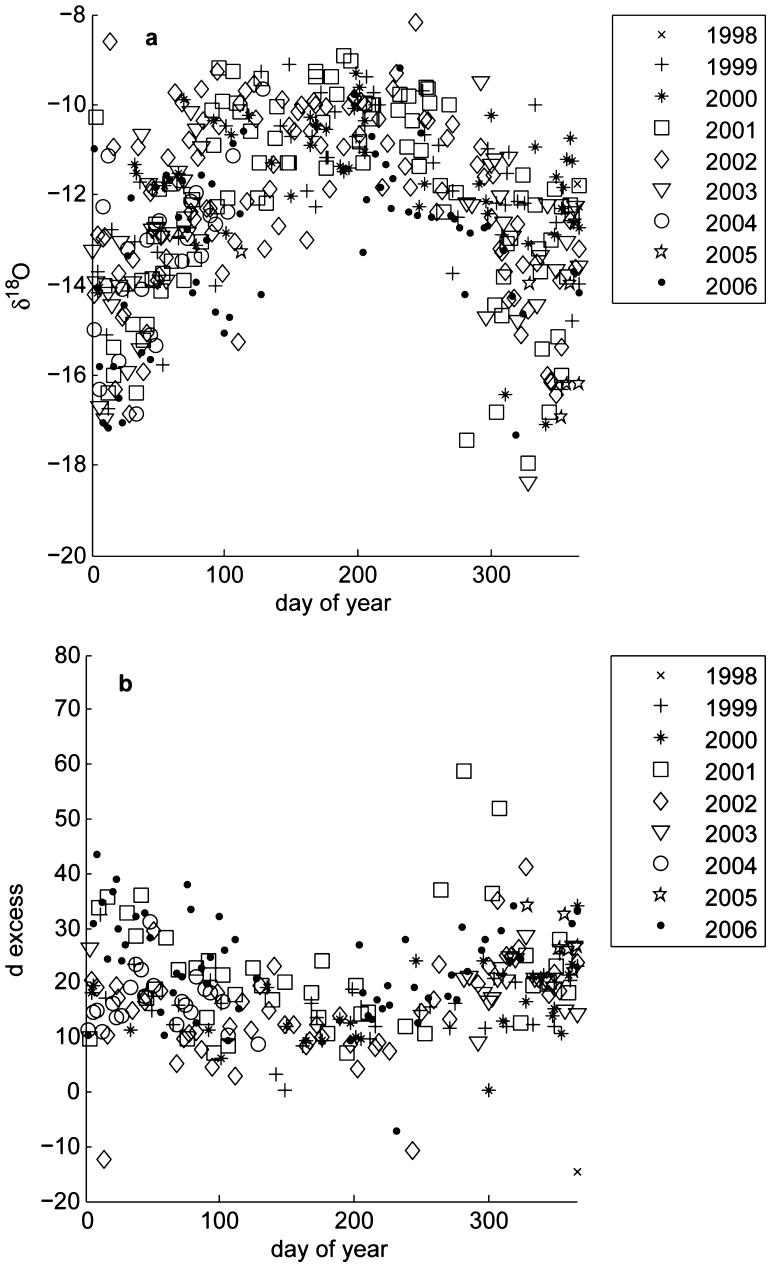

Fig. 3. Measured values (‰) of δ^{18}O (a) and δD (b) for the entire study period.

for the rainy season (October–May; Gat et al., 1994). A recent study in Greece (Argiriou and Lykoudis, 2006) reported a similar seasonal cycle in precipitation δ^{18}O over the entire year and attributed it to the depletion of the heavier isotopes by rain-out (colder temperature creates stronger rain-out). A similar control of temperature over the isotopic seasonal cycle was assumed by El-Asrag (El-Asrag, 2005) for Egypt. In the present study, we will discuss the seasonal cycle that we observed in the vapour isotopes, in contrast to precipitation in the previous studies. Although the rain-out effect will also be important in our study, some of the observed seasonal variations occur during the summer rainless periods (May–September), and thus, are not related to this effect. In addition, we will discuss here the role of vertical mixing and its effect on the vapour isotopes.

As noted in an earlier study that explored the first data in our data set (Gat et al., 2005), the vapour δ^{18}O approached the equilibrium value for the prevailing surface temperature on rainy days. In that study, examining selected sampling dates found relationships between the air mass trajectory and the observed isotopic composition. It was also noted that days with marked changes in the height of the inversion layer were accompanied by sharp changes in the vapour isotopic composition. Here we

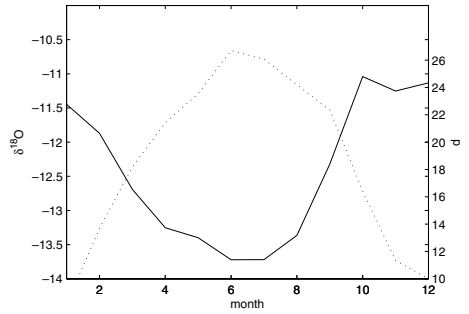

Fig. 4. The mean seasonal cycle values (‰) of δ^{18}O (dotted line) and deuterium excess (solid line).

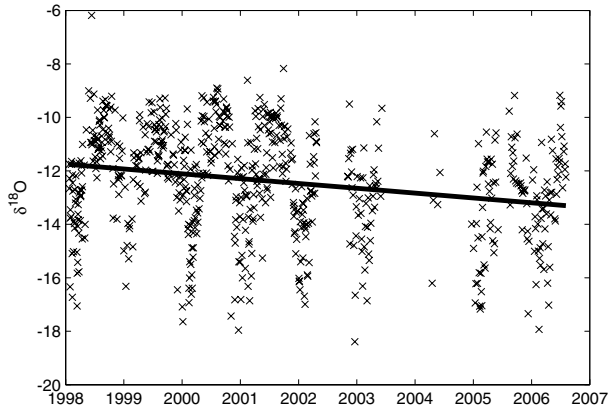

Fig. 5. The annual mean vapour δ^{18}O values (‰) and a trend line.

focused on the mean monthly values, specifically on the mean vapour isotopes' seasonal cycle and deviations from it, as well as on the longer timescale trends.

3.2. Is there a long-time trend in the vapour isotopes?

Plot of our entire data set versus time (Fig. 5) shows a clear trend of decreased δ^{18}O over the 9-year measurement period. Over this time frame, strong warming was observed over the eastern Mediterranean, a warming that is considerably stronger than the global warming for this time frame (Ziv et al., 2005; Alpert et al., 2006). Is the trend in vapour isotopes real, and if so, is it related to the temperature trend?

Because vapour sampling for this study was carried out with a varied number of hours per sampling day, we checked for the possible effect of sampling duration. There was no correlation between individual samples' collection times and δ^{18}O ($r = -0.06$). However, the annual mean δ^{18}O revealed a strong negative correlation with the annual mean collection duration ($r = -0.87$). Even if we exclude the rare samples with collection times exceeding 8 h and less than 6.5 h (Fig. 6), a strong correlation with δ^{18}O ($r = -0.81$) and δD ($r = -0.66$) exists. This effect cannot result from decreased efficiency in the collection system over time since such an effect would result in the

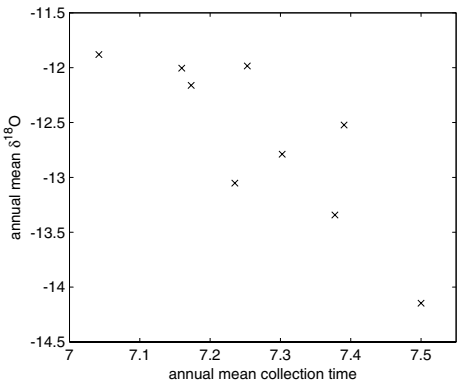

Fig. 6. The relationship between the annual mean collection time (in hours) for all years of study and the annual mean δ^{18}O (‰).

opposite trend (heavy isotopes preferentially condensed with decreasing efficiency over time).

Why is an effect of sampling time manifested only in the annual mean values? It is likely that other effects, such as synoptic variability (on the days-to-weeks timescale) and seasonal variation (on the longer scale) dominate over the effect introduced by change in sampling time. Only when we averaged all other effects, did this smaller sampling effect become evident. But this leads to the question of how can sampling time influence the isotopic composition of the collected vapour?

The observed trend can probably be explained by the daily cycle in near-surface turbulence. The collection started at 8 a.m. and ended between 12 p.m. and 4 p.m., when the boundary layer is turbulent. The morning hours (especially in winter) are characterized by lingering nocturnal inversion, with typical low wind speeds and, in turn, slow mixing of surface vapour with that from aloft (which has a lighter isotopic composition, see the following discussion). Warming of the ground by solar radiation during the day increases turbulence and mixing in the afternoon. In the summer, there is also a typical sea breeze front that reaches our sampling site in the late morning (Alpert and Rabinovich-Hadar, 2003) and further increases turbulence. The increased turbulence along the daily cycle is expected to mix down vapour with lighter isotopic composition and could create the apparent link between longer sampling time (a higher proportion of afternoon vapour) and lower delta values. Indeed, such an afternoon decrease in δ^{18}O was observed in an earlier study in the same region (Yakir, 1997).

The significance of the small variations in sampling time (even $^1/_2$ h) made it impossible to draw conclusions regarding interannual variability or long-time trends in our 9-year data set. Future studies should consider such an effect when determining a sampling strategy (e.g. using a full 24 h cycle, or the newly available diode-laser systems for real-time measurements). The isotope-enabled GCM run we have used was configured only to output monthly mean values. It would also be interesting to perform runs with hourly output to study how well the model captures the diurnal stability variability.

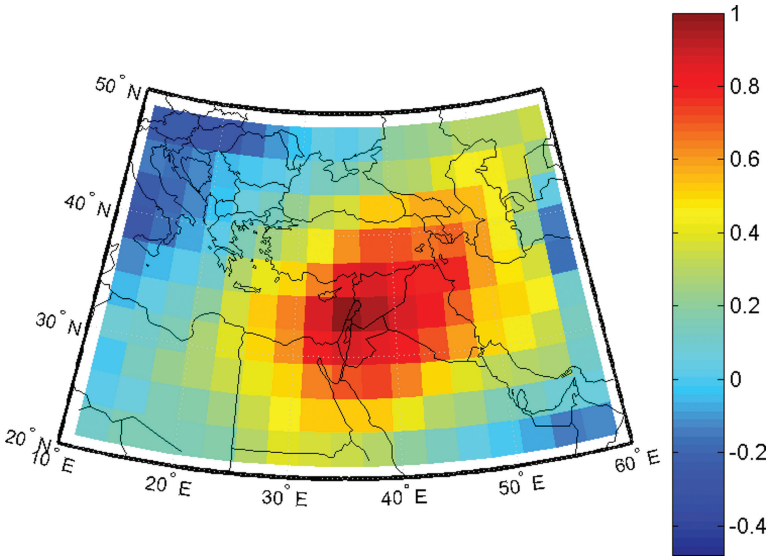

Fig. 7. Map of correlation (r) between interannual variability in vapour for the grid cell that covers the study area and the variability in nearby regions.

Notably, there was no relationship between sampling duration and month of year, and as a result, the mean monthly values are not correlated ($r = -0.12$) with the mean monthly collection time. Thus, there was no effect of sampling duration on the seasonal cycle, which is the focus of the discussion below. Further, the sampling time effect points out the potential significance of the vertical mixing (which changes during the day) for the isotopic composition of atmospheric water vapour, as will also be discussed in the context of the mean seasonal cycle.

3.3. Do observations in Israel represent the eastern Mediterranean region?

An important question regarding the usefulness for our observations for regional-scale studies is whether variations in the vapour isotopes at the sampling site in Israel represent well the vapour isotopes' variability over the EM and neighbouring areas. Since observations from other sites in the area are scarce, we addressed this question by utilizing the GCM output of monthly mean δ^{18}O in vapour. This is done assuming that the broad representation of the atmospheric mixing and other processes is captured well by the model, irrespective of the details of the isotopic variability. This is supported by the model's ability to simulate the study region's precipitation seasonality and large-scale spatial distribution of stable isotopes in meteoric water on regional and global scales (Lee et al., 2007).

We extracted a grid-cell from the model output, which covered our sampling area (centre of grid-cell at 32°N, 33.75°E) and compared the seasonal and interannual (after removing the seasonal mean) variability in this grid-cell to the variability in other neighbouring grid-cells. The results show good correlation ($r > 0.8$) in the seasonal timescale over most of the mid-latitudes, which is probably the result of the broad seasonal temperature changes over the entire Northern Hemisphere. More important, we also found a strong correlation ($r > 0.7$) between interannual variability in the local grid-cell and the rest of the EM and a weaker correlation ($r > 0.5$) with boarder areas (Fig. 7). This correlation at the interannual timescale indicates that the same controlling factors, working on synoptic scales, are responsible for the variability over Israel and adjacent areas. Therefore, at least, according to the isotope-enabled GCM and for our study region, measuring vapour isotopic composition at a single site is very useful for understanding variations in the isotopic composition of the vapour over a large region. Although local scale effects, not captured by the model, may be important in some cases, sampling far from the vapour sources of soil and vegetation (the roof top in our case), and at times when the vertical mixing is sufficient (see previous section) can ensure that a signal with a regional footprint is captured.

3.4 What controls the mean seasonal cycle of ^{18}O?

When considering the vapour δ^{18}O seasonality in the EM, a major factor that should be considered is the effect of removing heavy isotopes by precipitation. Since precipitation occurs in this area only in winter, it will tend to induce a lighter isotopic composition in the winter vapour, as in the observed seasonal cycle. Indeed, the vapour δ^{18}O seasonal cycle (monthly mean) is similar to the precipitation seasonal cycle (monthly mean) and the correlation between the two is considerable ($R^2 = 0.85$). However, comparing the seasonal march of δ^{18}O and amounts of rain shows (both in the mean monthly values in Fig. 4 and in individual years in Fig. 3a) variations of ~1 ‰ in δ^{18}O from May to September. In contrast, rainfall is almost absent from May to September, producing a seasonal cycle distinct from that of the vapour isotopes (Fig. 2). Thus, additional mechanisms must contribute to the isotopic seasonal cycle.

One of these additional mechanisms is related to the summer synoptic conditions in our study area. In the summer months, the EM is subject to two primary factors: mid-upper level subsidence, which contributes to warming, and lower level cool advection from the northwest. The subsidence is associated with the downward branch of both the Asian Monsoon and the Hadley cell across northern Africa (Ziv et al., 2004). The advection is associated with the Etesian winds, which are generated from a combination of the Persian Trough and the subtropical anticyclone of the Atlantic (Azores; Metaxas, 1977). The balance between the warming due to subsidence and cooling by advection controls the surface temperature during the summer in this region. As we will discuss further next, these circulation patterns probably have a significant impact on the atmospheric vapour isotopic composition.

The vertical profiles of vapour isotopes usually show depletion in the heavy isotopes with altitude, resulting from dehydration associated with the preferred condensation of the heavy isotopes (Ehhalt, 1974; Webster and Heymsfield, 2003). The coupling between the vapour isotopes and the synoptic conditions in our study site is hypothized to influence the seasonal cycle as follows:

In summer, the strong subsidence can have two opposing effects on the vapour isotopes. First, the subsiding air carries with it moisture from higher elevations, with its characteristic lower δ^{18}O, to the top of the planetary boundary layer (PBL). Second, the subsidence creates a thermal inversion that contributes to the atmospheric stability prevailing in summer. This will tend to increase the isotopic gradient in the PBL, since moisture from aloft with low δ^{18}O values mixes slower into lower layers. This pattern is in contrast to the winter pattern, which is characterized by more intense convective mixing. Thus, during summer, the subsidence effect tends to decrease the δ^{18}O of vapour in the PBL and the stability effect tends to increase it.

Support for our hypothesis, presented above, is given by two lines of observations. The first is temperature measurements at our site. The observations showed that the isotopes' seasonal cycle leads the seasonal cycle in surface temperature by a month (Fig. 8a). This is a strong indication that surface effects (associated with evaporation) are not the dominant control in this context. Further, a delay in the temperature seasonal march is expected if the surface temperature reacts slowly to the warming effect of the subsidence, and vice versa during cooling, probably mostly because of the large heat capacity of the Mediterranean Sea. In contrast, the effect of subsidence on the vapour isotopes is expected to be almost instantaneous, since the increase in stability prevents isotopically depleted moisture from aloft to be mixed downwards into the PBL.

Second, further support for our vertical mixing hypothesis and our interpretations of the seasonal delay of the temperature comes from the comparison of climatological means (for the region 31.25°N–38.75°N, 26.25°E–33.75°E) of the vertical wind velocities at 700 hPa pressure level (above the PBL) and the surface temperature (Fig. 8b, data source: NCEP–NCAR reanalysis). This shows a similar lag of about a month between the vertical wind component and surface temperature. This finding also supports the notion that the earlier seasonal rise in δ^{18}O is driven by subsidence and the marked seasonal changes in vertical mixing.

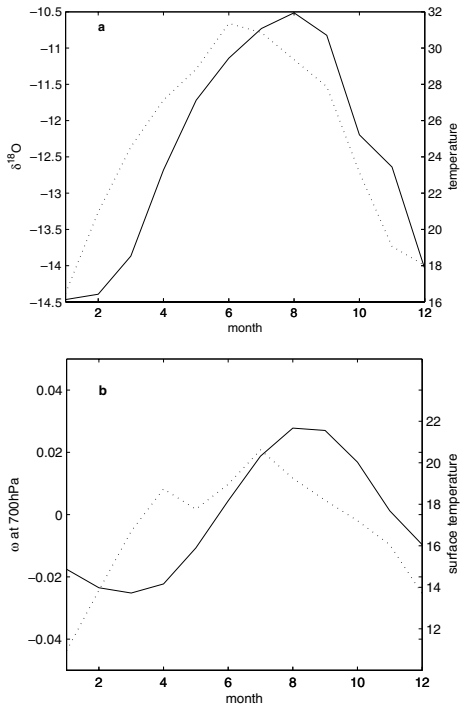

Fig. 8. (a) Mean seasonal cycle of δ^{18}O (dotted line) and surface temperature (°C, solid line). (b) Seasonal cycle of vertical wind (m s^{-1}) at 700 hPa (dotted line) and surface temperature (°C, solid line), (both from NCEP–NCAR reanalysis).

Changes in the isotopic composition of the initial vapour formed above the sea on a seasonal timescale can also affect δ^{18}O seasonality and must be considered. This effect will be considered quantitatively, together the vertical mixing effect, in the next section.

3.5. A semi-quantitative estimate of the possible contributions to the seasonal cycle

In this section, we will evaluate the contribution of the following mechanisms to the observed seasonal cycle: (1) changes in the flux of moisture from aloft and (2) changes in the initial vapour formed above the sea. The magnitude of the vapour isotopes' variability because of these two mechanisms will be compared with the magnitude of the variability associated with the seasonal cycle. This will allow us to assess whether the contribution of these two processes is important compared with the rain-out effects, which probably produce the primary isotopic seasonality.

We will begin our discussion by noting that the isotopic composition of the initial vapour formed above the sea is influenced,

first by the combined effects of sea surface temperature during evaporation, via its effect on the equilibrium fractionation factor and second, by the relative humidity, via its effect on the kinetic fractionation. First, we will consider the effect of change in relative humidity (RH) on the initial vapour. It has long been proposed that the large d values measured in winter at the EM must result from mixing of water vapour with maritime properties (low d) with vapour having very high d, formed at the continent lee-side. This high d is due, in turn, to rapid evaporation from the relatively warm sea to the cold and dry continental air (Gat et al., 2003). If this is the case, then the d seasonal cycle should be mainly controlled by seasonal cycle in RH.

What is the range of seasonal variability in surface RH over the EM? According to NCEP–NCAR reanalysis (Kalnay et al., 1996), the seasonal range is only 1%, which, according to the Craig–Gordon model, will have only a minor effect on variability of vapour isotopes and its d. However, the relevant processes in the Craig–Gordon model occur very close to the 'skin' layer of the sea surface, which is closer to the ocean than the NCEP–NCAR 'surface' layer. Thus, the Craig–Gordon equation requires, in fact, that the relative humidity will be normalized to that of the water surface temperature. Using the difference between the skin (sea surface) and surface air temperature (both derived from the NCEP–NCAR reanalysis), we estimated the skin relative humidity to be ∼80% in summer and ∼70% in winter. Indeed, low surface RH was measured in the winter season over the Mediterranean (Gat et al., 2003).

We used our estimates of RH variations between winter and summer in the steady-state model of Merlivat and Jouzel (1979), which follows the Craig and Gordon (1965) formulation for evaporation

$$ {}^{x}R_{V0} = \frac{{}^{x}\alpha_{ks}^{x}\alpha_{vl}^{x}R_{sea}}{1 - h_s + {}^{x}\alpha_{ks}h_s}, \quad (1) $$

where R the ratio of the heavy to light isotope, x denotes the heavy isotope and can be either 18 or 2, ${}^{x}\alpha_{ks}$ is the kinetic fractionation factor associated with evaporation from the ocean, ${}^{x}\alpha_{vl}$ is the equilibrium fractionation of vapour relative to liquid, ${}^{x}R_{sea}$ is the isotopic composition of seawater and h_s is the mean relative humidity over the ocean.

This model showed that the above RH range will drive a seasonal range of 5 ‰ in the d, which is comparable to the observed change. This same variability in RH will contribute only 0.7 ‰ to the δ^{18}O seasonal cycle, in comparison with a seasonal range of ∼3.5‰. The model above is based on the simplifying assumption that the initial vapour formed above the sea has its isotopic composition produced by a net evaporative flux. This means that vapour arriving at our sampling site does not contain any possible 'memory' of earlier evaporation/condensation effects. This first-order assumption is considered generally true in subtropical areas (Lee et al., 2007).

We can now use the same model and consider what range of skin temperatures (from 15 to 30 °C, the observed range of sea-surface temperatures in the EM) will be added to the seasonal variability in addition to the RH contribution. This calculation shows that the temperature effect results in an additional ∼1.1‰ contribution to the vapour δ^{18}O seasonal variation, which is observed to be 3.5‰. As expected, surface temperature variations had only a negligible effect (0.1 ‰) on the d values.

We will now estimate the effect of the seasonal variability in the flux from above the PBL on the isotopic composition of near-surface vapour. Although air from above the PBL is dry and delivers only small amounts of moisture into the PBL, the large isotopic depletion expected in this moisture can result in a discernible effect on the PBL isotopic ratios. To gain a first-order estimate, we used a simple isotopic mixing model. This model showed that a mix containing 5% moisture from aloft with δ^{18}O (−27) and δD (−220) (values taken from the GCM run for the layer above the PBL) and 95% initial winter surface vapour, with values calculated in the previous paragraphs, will have a vapour δ^{18}O shift of 0.7 ‰ relative to the initial vapour. The observed seasonal cycle is 3.5 ‰, thus this contribution cannot be ignored. There will also be a small contribution (0.6 ‰) to the d seasonal cycle because of the slight increase in this parameter with altitude. This slight increase in the d is due to non-linearity in the d definition, which cause it to slightly shift when there is a large decrease in δ^{18}O and δD (Gat et al., 1996). Our calculation show that mixing small amounts of vapour from aloft into the PBL can have an effect on the PBL vapour δ^{18}O cycle. However, does the flux of vapour into the PBL deliver such relatively small amounts?

To answer this question, we must estimate the size of the water vapour flux into and out of the PBL. Turbulent mixing in general, and particularly in the boundary layer, is difficult to model. However, we can take advantage of the monthly timescale we consider here. Over such a timescale, one does not need to deal with the daily changes in the PBL, but can use instead, a convenient approach based on the concept of 'Equilibrium PBL'. This concept has been developed and used (Betts and Ridgway, 1989; Helliker et al., 2004) to calculate the CO_2 exchange between the PBL and the free troposphere. According to this concept, when averaging over long time periods (e.g. a month), the PBL can be effectively treated by a 1-box model, with inputs and outputs only from the top and bottom. Differences in the incoming and outgoing horizontal fluxes are assumed to be small and are smoothed out by the temporal averaging. As a result, the water balance in the PBL is treated as a simple balance between moisture introduced by evaporation and moisture removed through mixing, into the free atmosphere (Helliker et al., 2004).

$$ F = r\rho W(q_p - q_t), \quad (2) $$

where F is the evaporative flux, ρ is the air density, W is the effective mixing velocity and q_p and q_t are the water vapour concentrations in the PBL and free atmosphere, respectively.

We have extracted from the NCEP–NCAR reanalysis data set the climatological surface latent heat flux and the water mixing

ratios at the surface and at 700 hPa. These values were used to estimate F, q_p and q_t. Using these parameters for January, which is taken to represent winter conditions, we can solve eq. (1) for the mixing velocity W. We can now write the (approximate) isotopic mass balance,

$$\delta_f F = \rho W(\delta_p q_p - \delta_t q_t), \tag{3}$$

where δ_f, δ_p and δ_t stand for the isotopic composition (for either δ^{18}O, δD, or d) of the evaporative flux, the PBL moisture and the free troposphere, respectively. Using the δ_f value as estimated above for the winter (i.e. with a RH of 70% and a sea-surface temperature of 15 °C) and the values of isotopic composition of the free troposphere taken from the GCM at 700 hPa, together with the reanalysis data, we can solve eq. (2) for the expected isotopic composition of the PBL, δ_t. According to this calculation, the flux of depleted vapour from aloft will result in reduction of the surface vapour δ^{18}O in the order of 6‰, in winter.

This is, of course, a considerable effect. In summer, the more stable PBL will prevent much of the depleted vapour from reaching the surface. Currently, we cannot estimate this variability in mixing within the PBL, but considering that the isotopic flux into the top of the PBL is large, even a small variation of this flux will have a significant impact on the surface vapour isotopic composition.

However, there are some caveats with our estimate. First, the isotopic values of the free atmosphere were taken from the GCM run, which is not constrained by measured values (which are unavailable). Second, a large uncertainty is associated with the evaporative flux (Helliker et al., 2004). And last, the assumption that all the vapour originating either from the EM sea surface or from aloft, is over-simplistic. Nevertheless, our calculation shows that the isotopic flux created by depleted vapour entraining the PBL cannot be neglected.

3.6. Model-observations comparison

Our comparison of the vapour observation with the model showed that, surprisingly, the isotope-enabled GCM fails in predicting the δ^{18}O seasonal cycle over the EM (Fig. 9) and predicts an almost completely off-phase seasonal cycle. However, the model correctly predicts the phasing of precipitation over the area (not shown); therefore, the interaction of vapour with rain cannot be the main cause for the observed discrepancy. The incorrect phasing of the δ^{18}O seasonal cycle was accompanied, as might be expected, by incorrect phasing of the deuterium-excess (not shown), which is known to be a harder parameter to model.

One possible explanation for the δ^{18}O discrepancy in the model observations might be the model's failure in estimating the contrasting effect of the summer's subsidence on the one hand and the summer's stronger vertical stability on the other. Therefore, either the subsidence in the model is too high or the subsiding air has too low values of δ^{18}O.

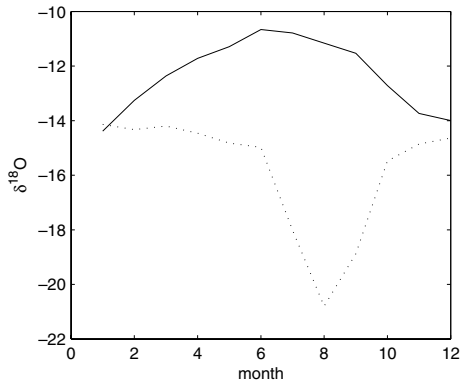

Fig. 9. Modelled (dotted line) and measured (solid line) mean seasonal cycle of δ^{18}O.

This later problem may stem from the fact that the water vapour in subtropical upper atmosphere comes from tropical upper atmosphere. Tropical upper atmospheric water vapour has a higher δ^{18}O value than the values expected from the Rayleigh distillation model because of the entrainment, convective mixing and evaporation of the detrained water (Lee et al., 2008). If a model creates an incorrect entrainment and/or evaporation of detrained water over tropics, the δ^{18}O value of water vapour at the subtropical upper atmosphere will also be incorrect. Further investigations will be aimed at determining why the GCM we have used (CAM2.0), failed in simulating the seasonal cycle. Irrespective of the explanation, the model versus measurements' discrepancy illustrates the critical need for vapour isotope measurements, in addition to traditional meteorological and precipitation isotope measurements to validate and improve GCMs.

4. Conclusions

Using a long-term data set, we characterized the seasonal cycle in the EM atmospheric vapour isotopic composition. Using the model, reanalysis data and simple budget calculations, we estimated that the observed seasonal cycle of vapour isotopes is influenced by temperature and RH-driven isotopic variability in the initial vapour and by the potentially large effect of varying the flux of depleted moisture from aloft. We concluded that these factors, superimposed on the well-described rain-out effect, produce the observed seasonal cycle and control the interannual variations associated with it.

The failure of the isotope-enabled GCM in capturing the seasonal cycle at our site illustrates the importance of vapour isotope observations as a tool for constraining GCMs. In this respect, the results also indicated the importance of a sampling strategy that carefully considers the short-time, diurnal variations in vapour isotopes.

5. Acknowledgments

We thank Joel Gat for valuable discussions and two anonymous reviewers for comments on an earlier version of this manuscript.

AA was supported by a postdoctoral Fellowship from the Feinberg Graduate School, the Weizmann Institute of Science. Financial support from the Minerva foundation and the BSF is gratefully acknowledged.

References

Alpert, P. and Rabinovich-Hadar, M. 2003. Pre- and post-sea-breeze frontal lines – a meso-gamma-scale analysis over south Israel. *J. Atmos. Sci.* **60**, 2994–3008.

Alpert, P., Krichak, S. O., Dayan, M. and Shafir, H. 2006. Climatic trends over the eastern Mediterranean: past and future projections. *CLIVAR Exchanges* **37**, 12–13.

Argiriou, A. A. and Lykoudis, S. 2006. Isotopic composition of precipitation in Greece. *J. Hydrol.* **327**, 486–495.

Ayalon, A., Bar-Matthews, M. and Sass, E. 1998. Rainfall-recharge relationships within a karstic terrain in the eastern Mediterranean semi-arid region, Israel. *J. Hydrol.* **207**, 18–31.

Bender, M., Sowers, T. and Labeyrie, L. 1994. The Dole effect and its variations during the last 130,000 years as measured in the Vostok ice core. *Global Biogeochem. Cycles* **8**, 363–376.

Betts, A. K. and Ridgway, W. 1989. Climatic equilibrium of the atmospheric convective boundary-layer over a tropical ocean. *J. Atmos. Sci.* **46**, 2621–2641.

Bolin, B. 1958. On the use of tritium as a tracer for water in nature. In: *Proceedings of the Second International Conference on Peaceful Use of Atomic Energy*, Geneva, 1958.

Chen, M., Xie, P., Janowiak, J. E. and Arkin, P. A. 2002. Global land precipiation: a 50-yr monthly analysis based on gauge observations. *J. Hydrometeorol.* **3**, 249–266.

Collins, W. D., Hack, J. J., Boville, B. A., Rasch, P. J., Williamson, D. L. and co-authors. 2002. *Description of the NCAR Community Atmospheric Model (CAM2)*. NCAR, Boulder, 189pp.

Craig, H. and Gordon L. I. 1965 Deuterium and oxygen-18 variations in the ocean and the marine atmosphere. In: *Proceedings of a Conference on Stable Isotopes in Oceanographic Studies and Paleotemperatures* (ed.E. Tongiorgi). Spoleto, Italy, 9–130.

Dai, A., Fung, I. and DelGenio, A. D. 1997. Surface observed global land precipitation variability during 1900–1988. *J. Clim.* **10**, 2943–2962.

Dansgaard, W. 1964. Stable isotopes in precipitation. *Tellus* **16**, 436–468.

Ehhalt, D. H. 1974. *Vertical profiles of HTO, HDO and H2O in the troposphere*. NCAR, Boulder, CO, 1–131.

El-Asrag, A. M. 2005. *Effect of synoptic and climatic situations on fractionation of stable isotopes in rainwater over Egypt and east Mediterranean*. IAEA, Vienna, 51–73.

Farquhar, G. D., Lloyd, J., Taylor, J. A., Flanagan, L. B., Syvertsen, J. P. and co-authors. 1993. Vegetation effects on the isotope composition of oxygen in atmospheric CO (sub 2). *Nature* **363**, 439–443.

Gat, J. R. 1987. Variability (in time) of the isotopic composition of precipitation: consequences regarding the isotopic composition of hydrologic systems. In: *Use of isotope techniques in water resources development*. IAEA, Vienna, 551–563.

Gat, J. R. and Dansgaard, W. 1972. Stable isotope survey of freshwater occurrences in Israel and the Jordan Rift Valley. *J. Hydrol.* **16**, 177–211.

Gat, J. R., Carmi, I. and Bauman, N. 1994. The isotopic composition of precipitation at Bet-Dagan, Israel: the climatic record (1961–1990). *Israel Meteorol. Res. Papers* **5**, 10–19.

Gat, J. R., Shemesh, A., Tziperman, E., Hecht, A., Georgopoulos, D. and co-authors. 1996. The stable isotope composition of waters of the eastern Mediterranean Sea. *J. Geophys. Res.-Oceans* **101**, 6441–6451.

Gat, J. R., Adar, E. and Alpert, P. 2001. Inter- and intra storm variability of the isotope composition of precipitation in southern Israel: are local or large scale factors responsible? In: *Proceedings of the international conference on the study of environmental change using isotope techniques*, Vienna, 2001.

Gat, J. R., Klein, B., Kushnir, Y., Roether, W., Wernli, H. and co-authors. 2003. Isotope composition of air moisture over the Mediterranean Sea: an index of the air-sea interaction pattern. *Tellus* **55B**, 953–965.

Gat, J. R., Ben-Mair, R., Yama, R., Yakir, D. and Wernli, H. 2005. *The Isotope Composition of Atmospheric Waters in Israel's Coastal Plain*. IAEA, Vienna, 99–114.

Goodfriend, G. A., Magaritz, M. and Gat, J. R. 1989. Stable isotope composition of land snail body water and its relation to environmental waters and shell carbonate. *Geochimica et Cosmochimica Acta* **53**, 3215–3223.

Helliker, B. R., Berry, J. A., Betts, A. K., Bakwin, P. S., Davis, K. J. and co-authors. 2004. Estimates of net CO_2 flux by application of equilibrium boundary layer concepts to CO_2 and water vapor measurements from a tall tower. *J. Geophys. Res.-Atmos.* **109**, doi:10.1029/2004JD004532.

Hoffmann, G., Jouzel, J. and Masson, V. 2000. Stable water isotopes in atmospheric general circulation models. *Hydrol. Proc.* **14**, 1385–1406.

Jouzel, J. and Merlivat, L. 1984. Deuterium and O-18 in precipitation – modeling of the isotopic effects during snow formation. *J. Geophys. Res.-Atmos.* **89**, 1749–1757.

Kalnay, E., Kanamitsu, M., Kistler, R., Collins, W., Deaven, D. and co-authors. 1996. The NCEP/NCAR 40-year reanalysis project. *Bull. Am. Meteorol. Soc.* **77**, 437–471.

Lee, J. E. 2005. *Atmospheric water: perspectives from isotopes and the NCAR climate model*. PhD Thesis, University of California, Berkeley.

Lee, J. E. and Fung, I. 2008. Amount effect of water isotopes and quantitative analysis of post-condensation processes. *Hydrological Processes* **22**(1), 1–8.

Lee, J. E., Fung, I., DePaolo, D. J. and Henning, C. 2007. Analysis of the global distribution of water isotopes using the NCAR atmospheric general circulation model. *J. Geophys. Res* **112**, doi:10.1029/2006JD007657.

Lee, X., Sargent, S., Smith, R. and Tanner, B. 2005. In situ measurement of the water vapor O-18/O-16 isotope ratio for atmospheric and ecological applications. *J. Atmos. Oceanic Technol.* **22**, 555–565.

Leguy, C., Rindsberger, M., Zangwil, M., Issar, A. and Gat, J. R. 1983. The relation between the oxygen-18 and deuterium contents of rainwater in the Negev Highlands and air mass trajectories. *Isotope Geosci.* **1**, 205–218.

Levin, M., Gat, J. R. and Issar, A. 1980. Precipitation, flood and groundwaters of the Negev Highlands: an isotopic study of desert hydrology. In: *Arid Zone Hydrology; Investigations with Isotope Techniques*. IAEA – AG, Vienna, 3–23.

Mathieu, R., Pollard, D., Cole, J. E., White, J. W. C., Webb, R. S. and co-authors. 2002. Simulation of stable water isotopevariations by

the GENESIS GCM for modern conditions. *J. Geophys. Res.* **D107**, 2–18.

Merlivat, L. and Jouzel, J. 1979. Global climatic interpretation of the deuterium-oxygen-18 relationship for precipitation. *J. Geophys. Res.-Oceans Atmos.* **84**, 5029–5033.

Metaxas, D. A. 1977. The interannual variability of the Etesian frequency as a response of atmospheric circulation anomalies. *Bull. Hellenic Meteorol. Soc.* **2**, 30–40.

Rozanski, K. and Sonntag, C. 1982. Vertical-distribution of deuterium in atmospheric water-vapor. *Tellus* **34**, 135–141.

Tzur, Y. 1971. *Isotope effects in the evaporation of water into air*. Ph.D. Thesis, The Weizmann Institute of Science, Rehovot.

Webster, C. R. and Heymsfield, A. J. 2003. Water isotope ratios D/H, 18O/16O, 17O/16O in and out of clouds map dehydration pathways. *Science* **302**, 1742–1745.

Yakir, D. 1997. Oxygen-18 of leaf water: a crossroad for plant-associated isotopic signals. In: *Stable Isotopes and the Integration of Biological, Ecological and Geochemical Processes* (ed.H. Griffiths), Oxford, 147–168.

Zhang, G. J. and McFarlane, N. A. 1995. Sensitivity of climate simulations to the parameterization of cumulus convection in the canadian climate center general-circulation model. *Atmos. Ocean* **33**, 407–446.

Ziv, B., Saaroni, H. and Alpert, P. 2004. The factors governing the summer regime of the eastern Mediterranean. *Int. J. Climatol.* **24**, 1859–1871.

Ziv, B., Saaroni, H., Baharad, A., Yekutieli, D. and Alpert, P. 2005. Indications for aggravation in summer heat conditions over the Mediterranean Basin. *Geophys. Res. Lett.* **32**, L12706, doi:12710.11029/12005GL022796.